

Safe Evacuation Routes in Inundated Situations: Assessment of a Lowland District in Eastern Tokyo

Ko Inoue

Graduate School of Science and Engineering
Hosei University, Tokyo 184-8584, Japan
ko.inoue.9j@stu.hosei.ac.jp

Daiki Ito

LTS, Inc., Tokyo 107-0051, Japan
daiki.ito.1008@gmail.com

Daiki Okamura

Toho System Science Co., Ltd., Tokyo 112-0002, Japan
okamudaiki@gmail.com

Hiroyuki Goto

Department of Industrial and Systems Engineering
Hosei University, Tokyo 184-8584, Japan

Abstract

Finding a safe evacuation route is important in the event of an accident or natural disaster. Along with the climate change in recent years, torrential rains have become more occasional than before in both urban and rural areas. Intensive and continuing rainfall may lead to disasters such as landslides and inundations. Even if a single point on an evacuation route is inundated or critically damaged, then the route is unavailable and the evacuees who were planning to use it must find another route. In addition, in lowland districts in urban areas, where a large number of local people reside, might rush on limited available roads, particularly when a mandatory evacuation is alerted. This may raise another type of risk by excessive human flow or traffic congestion. Most hazard maps are created according to geographical elevations, which quantifies the extent of flood risk, typically in terms of inundation depth. Those kinds of maps may be useful for averting or mitigating property damage, while it is not tied with safeness of evacuation routes. In the case of an inundation in lowland areas, a large number of roads in the vicinity of rivers would become inundated and unavailable. This type of temporal risk due to congestion has not been considered to date. This study along this line considers both geographical elevations and availability of roads. A lowland district in eastern Tokyo, Adachi City, is focused on for an assessment. Empirical findings highlight the impact of traffic congestion and isolation of flooded areas.

Keywords

Inundation, congestion, evacuation, digital elevation model, lowland district.

1. Introduction

Along with the climate change in recent years, personal and property damages caused by extraordinary weathers such as torrential rains and furious typhoons have increased the necessity of risk re-assessment of river flooding and flood disaster. In the event of a sudden disaster such as flooding and landslide, prompt evacuation may aid avoiding or decreasing personal damage, while the shortest or shorter routes might not be available as evacuation routes. Not only natural disasters but also human flows might cause an accident or even lead to a disaster. For instance, the Itaewon

crowd accident occurred in South Korea in the year of 2022 brought us a significant impact. Crowd accidents might take place on evacuation routes.

Most hazard maps are created according to geographical or geometrical aspects, such as altitude or road width, the outlet of which highlights regions with higher risk of being damaged. However, the impact of traffic congestion or human flow of evacuees are not taken into account in such maps. Several prospective routes may unpredictably turn unavailable in disastrous situations, thereby hazard maps that reflect the impact of congestion might be considered to achieve fast and safe evacuation. Therefore, in this study, the impact of congestion is incorporated to seek evacuation routes, aiming to prevent further accidents and delays caused by excessive human flow.

2. Technical Background

2.1 Hazard Maps

Hazard maps are designed to help finding evacuation routes in disastrous circumstances. For example, the hazard map distributed by a city in eastern Tokyo (Adachi Ward, the study area) provides information on inundation height, evacuation sites in flood disasters, and major routes suited for evacuation. However, only with this kind of maps, it is hard to identify which route is appropriate to evacuate quickly and safely. Additionally, to avert accidents caused by increase of pedestrian flow and/or by traffic congestion, it is important to predict which roads can be congested. Encountering unpredictable congestions may result in retard in evacuation. This study along this line aims to incorporate the impact of traffic congestion, aiming the map to be effective in delineating flood inundation maps.

2.2 Congestion Calculation

Traffic flows are estimated along with several assumptions. A person or vehicle is assumed to choose the shortest route from a source point to a destination point. This is called a person-trip. A person moves along the selected path, along which a traffic for one person is recorded. The destination point can be any location across the network, on which a unit (or weighted if applicable) traffic load is accumulated for each trip. This is repeated for all source points in the network. To solve a single-source and all-destination paths problem, the Dijkstra's algorithm is applied in this study. Among others, an algorithm based on a min-priority queue is applied, in order to effectively reuse the outlets of the predecessor edges along the computed shortest routes. Starting from a destination point, traffic loads are accumulated on edges toward upstream (Goto et al. 2019; Cascetta and Nguyen 1988). The holistic accumulation of all-pair person trips comprises the estimated traffic congestion in the entire network.

2.3 Flood Simulation

Main targets in this study are lowlands in urban districts that are occasionally exposed to risks of flood damage by torrential rains. A flood simulation is conducted applying the method developed in Matsutani and Magome (2014), Kwak et al (2012), and Sayama et al. (2012). They are designed for creating a flood inundation map using Digital Elevation Model (DEM) datasets (Croneborg et al. 2015), which comprises the following procedures.

- Step F1: Assume a location of a levee breach along with the inundation depth, H . Then, determine the depth interval $\Delta h = H/N$ to simulate for varying depths, where N is a natural number. The breach position is assumed to be the point where the flood begins and inundation starts.
- Step F2: The elevation at the point of flooding is set to h_0 , and it is incremented by Δh . The updated elevation $h_0 + \Delta h$ turns into a new elevation, and is dealt with the water surface elevation.
- Step F3: Check the eight neighboring points of point i if or not they are flooded. If point j is unflooded and $h_i \leq h_j$ follows, then lift the elevation h_j by $\min[\Delta h, h_i - h_j]$ and label it as flooded. If there are multiple inundated points around point j , then set the increase of the elevation to the average of those differences. While possible, further change in the elevation of inundated points is not considered to avert inflation in the computation load.

Figure 1 demonstrates an example of inundation with $\Delta h = 2\text{m}$, where the values in the cells represent the elevations in meters. If the two cells in the left bottom (elevations 110 and 109) are inundated, then the three neighboring cells with thick lines (elevations 108, 105, and 104) are newly inundated. The two cells of 105 and 104 are adjacent to that of 109, for which their elevations are lifted by $\Delta h=2\text{m}$ ($<109-105=4$) and $\Delta h=2\text{m}$ ($<109-104=5$), respectively. The cell of 108 is adjacent to that of 110 and 109, thereby the average value of the two differences ($((110-108)+(109-108)/2)$) amounts to 1.5m. This value is added to the cell of 108. Note that the elevation of the inundated point (109) is lower than that of the adjacent inundated point (110), which is not lifted any further as mentioned in Step 3 above.

120	100	104	110
115	108	105	106
110	109	104	108
↓			
120	100	104	110
115	109.5	107	106
110	109	106	108

Figure 1. Example of inundation calculation

- Step F4: If a new inundation point is added in Step F3, repeat Step F3 for that point. By contrast, if there is no additional inundation point, record the entire inundated area at this stage, and set the elevation of water surface in the current inundated area as a ground elevation. Then return to Step F2. If the increase in elevation at the starting point of the flood has already reached H , then proceed to Step F5.
- Step F5: Overlay the N inundated areas created in Step F4 on the map. Given the location of the levee breach in Step F1, an estimated inundation area map is now complete.
- Step F6: If there are multiple breach locations, then overlay the inundation area maps created individually in Steps F1–F5.

3. Inundation Assessment

3.1 Study area

A lowland district in eastern Tokyo, Adachi Ward (hereafter this will be called Adachi City), is chosen as a study area, the location of which is identified in Figure 2. A major river in central Tokyo called the Arakawa River flows the southern part of the area.

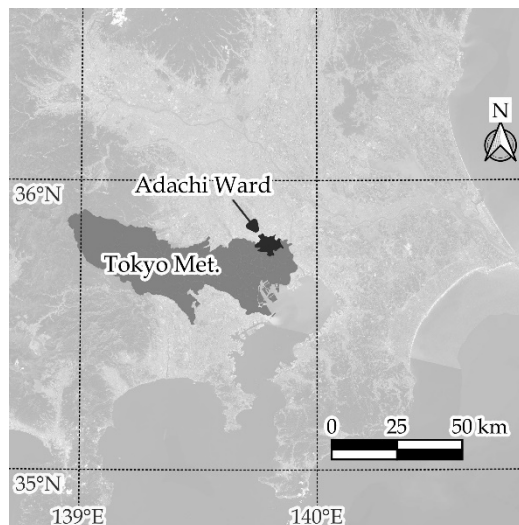


Figure 2. Study area (Adachi Ward, Tokyo)

3.2 Raster data for simulating inundation

A dataset distributed by The National Land Numerical Information Download Service called “Anticipated Flood Inundation Area” is used. Anticipated flooded areas when rivers overflow can be delineated using this dataset. However, due to its coarse resolution, the outlet inevitably becomes coarse when magnified. It is thus not practical when applying it to the scale of the entire city. Since congestion calculations along with other analyses are conducted for Adachi City, using this dataset would be inappropriate. Therefore, using datasets with higher resolution would be more adequate. In this study, Digital Elevation Model (DEM) data with a mesh size of 5m is used. This data for Adachi City can be retrieved from “Fundamental Geospatial Data” provided by the Geospatial Information Authority of Japan. It includes coordinates of the centroids of the mesh along with corresponding elevations.

3.3 Inundation simulation

In step F1 summarized in 2.3, we assume breach points along the river where floods occur, each point of which has the corresponding inundation depth. The depth H does not mean the height of embankment but refers to the final depth of water outflows from the embankment.

We select eight breach points and conduct simulations for each point with varying inundation depths $H=2, 4,$ and 6m . The selected breach points are located on the outer side of the curves along the Arakawa River, whereon they would have higher risks of embankment failure by erosion due to extensive waterflow. Of the eight breach points, five points are located on the northern side of the river, whereas three points on the southern side. In reality, however, the outer side of the embankments would be constructed in a solid manner to avert embankment failure. Thus, it is not surprising if breaches occur at any locations other than the eight points.

Inundation may be delayed at distant locations from the breach points. But in reality, the actual breach locations are unpredictable, and the arrival of flooding may significantly differ from the simulated results. Therefore, to achieve precise simulation, it could be optional to increase the number of breach points. However, this study must focus only on the selected eight breach points to accelerate computation.

We set the increment $\Delta h = 0.10\text{m}$, which will be fixed irrespective of H . Adachi City is a low-lying area with minimal variations in the surface topography. Since the mesh size of the data that will be used in this study is 5m, there would be no significant changes in elevation between neighboring meshes. With a smaller value of Δh , the variation in elevation within one iteration becomes smaller, enabling computations even in low-lying areas such as Adachi City. In Steps F2 and F3, we conduct simulations by incrementing the elevation at the eight selected breach points. It is important to note that the breach points and the elevation values after the changes at each location are dealt with as the elevation of water surface.

3.4 Flooded areas

Simulated flood areas with varying inundation depths are presented. Figures 3, 4, and 5 delineate the results for inundation depths $H=2, 4,$ and 6 , respectively. The colors used to signify the inundation depth are summarized in Table 1.

Table1. Colors used for delineation

Color	Inundation depth
White	0 m
Blue	< 0.5 m
Green	< 1.0 m
Yellow	< 1.5 m
Orange	< 2.0 m
Red	≥ 2.0 m

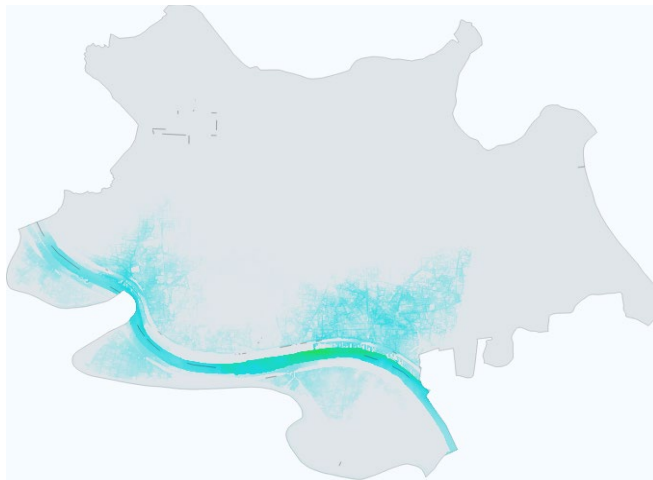


Figure 3. Flooded areas with inundation depth $H=2$

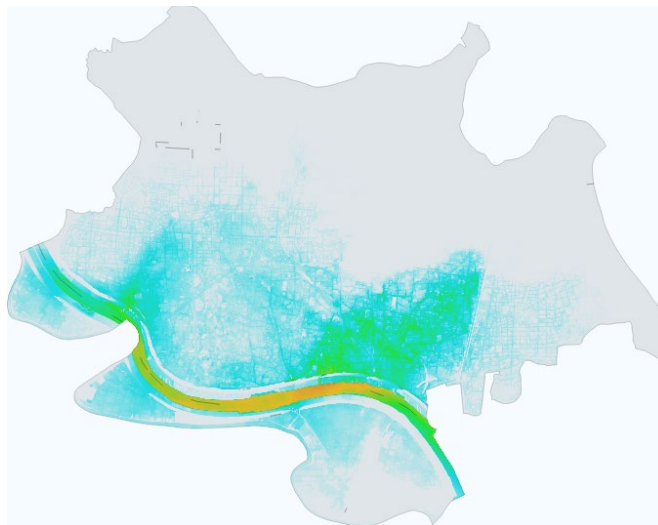


Figure 4. Flooded areas with inundation depth $H=4$

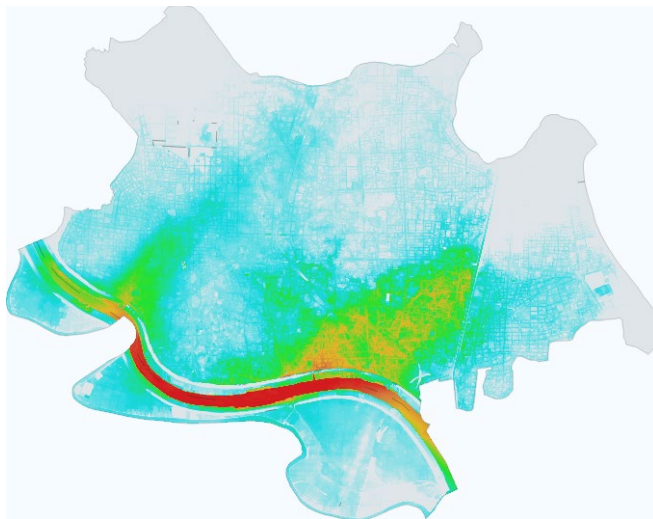


Figure 5. Flooded areas with inundation depth $H=6$

A close inspection of the northern side of the Arakawa River reveals that the inundation primarily spreads in the low-lying areas irrespective of the value of H . Particularly noticeable is the region slightly east of the western and central parts of Adachi City, indicating that the area around is a low-lying land. Although five breach points are set on the north side of the Arakawa River, the observed spread of water can be inferred that a change or increase of the number of breach points would not impact significantly overall.

Furthermore, in the eastern region on the north side of the river, a line dividing the water spread can be seen. A smaller amount of spreading water can be identified beyond the line. This division corresponds to the Ayase River flowing from the north to south in Adachi City. In the case of $H=6$, because of the Ayase River, the northeastern part of Adachi City experiences a delayed flooding. On the southern side of the river, most areas are low-lying land with elevations below 1m. Along with this topography, most areas are inundated in $H=4$ and 6. However, in the southwestern region where roads and railway tracks run along the embankment, the elevation of which is relatively higher than the surrounding areas, yields smaller probability of flooding.

4. Congestion Assessment

4.1 Vector data for congestion computation

The road network dataset used in this study is called “Geographical Survey Institute Map Vector Provision Experiment” distributed by the Conservation GIS Consortium Secretariat. Only the road network data in Adachi City was extracted. The extracted data includes various scales of roads including both arterial and minor ones. However, this originally contained approximately 100,000 intersections as nodes. Thus, to save the computation time, only the major roads were selected by which the number of nodes was reduced to approximately 600.

4.2 Simulated congestion

The congestion level is simulated by first solving an all-pair shortest path problem followed by accumulation of unit traffics on edges along the shortest path for all starting points (Goto et al. 2019; Goldberg 2001; Zhan and Noon. 1998). We overlay the flood inundation map to identify evacuation routes in a disastrous situation. Contrary to normal situations, people are expected to keep away from rivers in such situation. The congestion calculation focuses on nodes near the boundary of Adachi City, which play roles as destinations. As there are roads that would become unavailable upon flooding, we incur a constraint that enforces closure of the evacuation routes by overlaying the flooded areas. The shortest paths in a disaster are then determined in the flood inundation map. Congestion calculations are conducted assuming that the flooded roads are unavailable. Then, the road network is overlaid on the flood inundation maps. The procedures are summarized below.

- Step C1: Overlay the road network on a flood inundation map. Figure 6 delineates the resulting overlay for $H=2$.
- Step C2: Subtract unavailable road segments due to the simulated inundation. The subtracted network is used for the congestion assessment. Figure 7 presents the update by this operation.
- Step C3: Calculate the shortest paths for each destination using the Dijkstra's algorithm. Then accumulate unit traffic loads along the path.

4.3. Discussion

Let us have a closer look at the southern part of Adachi City. The bridges linking the southern and northern areas are unavailable due to the flood, for which the southern area comprises an isolated network. The orange lines indicate roads with higher traffic volumes, along with demarcation of traffics by thickness of the lines. Purple lines are roads with zero traffic volume. In Figures 8 and 9, a larger number of zero-congested roads are observed in the southern part. Since another river called the Sumida River flows further in the south of the southern area, there are few sites suited for evacuation. Thus, the flow of people would have concentrated on roads with short distances.

Next, focus on the northern part of Adachi City. Figure 8 ($H=2$) highlights higher congestion in the northwestern areas than the other areas. This would be because the city border is contiguous with adjacent cities, and there are fewer restrictions in selecting an evacuation route than the other areas. The selection may involve crossing a river in southern areas.



Figure 6. Overlay of the road network on the inundation map for $H=2$

This trend is also similar in Figure 9 ($H=4$); the congestion level is high in the northwestern part and there are many zero-congested roads particularly in the southeastern part. On the other hand, the arterial roads in the center are flooded, for which the major evacuation routes are moved northward compared with $H=2$. In Figure 10 ($H=6$), there are smaller number of available roads.



Figure 7. Road segments still available in the flooded situation

The evacuation routes are divided into east-west and west-west areas. The extent of congestion is less various than those for $H=2, 4$, while it remains high in the northwestern part. This would be because there are greater number of destinations.



Figure 8. Congestion simulation for inundation depth $H = 2$

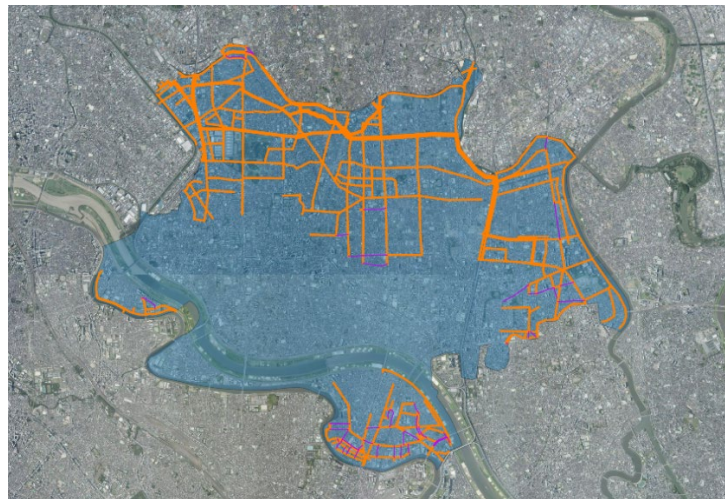


Figure 9. Congestion simulation for inundation depth $H = 4$

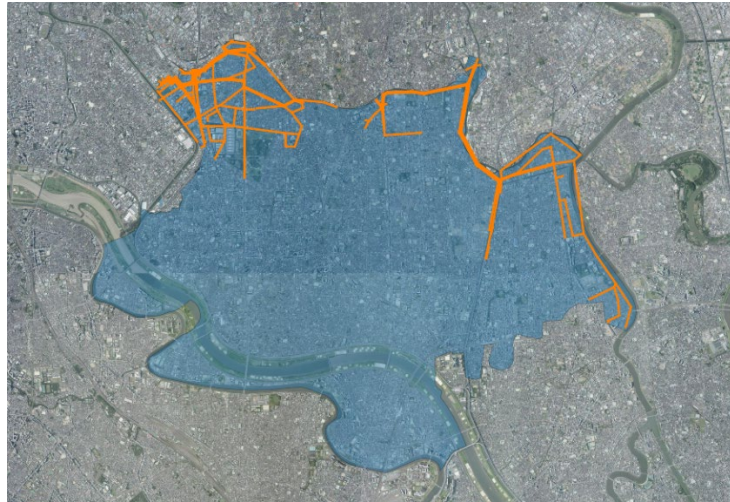


Figure 10. Congestion simulation for inundation depth $H = 6$

5. Conclusion

In this study, congestion calculations were conducted to create flood inundation maps. The main purpose of creating this map is to avert encountering accidents and delays in evacuation due to excessive human flow. The outlet may serve as new hazard maps. The results of the congestion computation indicate that even the impact by narrow streets is noticeable because the shortest routes are the most congested than the main streets. People who are familiar with minor roads around the area, such as local residents, can rush into shortcuts that have a higher risk of human and/or traffic accidents. Instead, evacuating using arterial road could avoid accidents associated with human flow. If the results of this study will be used as hazard maps, only the simulated congestion may be opened to public. The flow of people will be dispersed as evacuees reach their destinations, avoiding the routes with thicker lines with their judgment. In addition to the obtained inundation maps, it is necessary for each individual to be aware of existing hazard maps published by local governments. Non-flooded roads will help people avoiding from detour by encountering flooded areas, and will aid them to evacuate efficiently without increasing human flow. Future work may take into account data such as population distribution, road width, and number of lanes. Experiments using a more realistic number of roads may be conducted to obtain more detailed results.

References

- Cascetta, E. and Nguyen, S., A unified framework for estimating or updating origin/destination matrices from traffic counts, *Transportation Research Part B: Methodological*, vol. 22, no. 6, pp. 437–455, 1988.
- Croneborg, L., Saito, K., Matera, M., McKeown, D. and van Aardt, J., *Digital Elevation Models*, pp. 1–17, 2015.
- Goldberg, A.V., A simple shortest path algorithm with linear average time, *Proceedings of the 9th Annual European Symposium on Algorithms*, pp. 1–17, Aarhus, Denmark, August 28–31, 2001.
- Goto, H., Kakimoto, Y. and Shimakawa, Y., Lightweight computation of overlaid traffic flows by shortest origin-destination trips, *IEICE Transactions on Fundamentals of Electronics, Communications and Computer Science*, vol. E102-A, no. 1, pp. 320–323, 2019.
- Kwak, Y., Takeuchi, K., Fukami, K. and Magome, J., A new approach to flood risk assessment in Asia-Pacific region based on MRI-AGCM outputs, *Hydrological Research Letters*, vol. 6, pp. 70–75, 2012.
- Matsutani, K. and Magome, J., A simple prediction method of potential flooding area only using digital elevation model (In Japanese), *Theory and Applications of GIS*, vol. 22, no. 1, pp. 15–25, 2014.
- Sayama, T., Ozawa, G., Kawakami, T., Nabesaka, S. and Fukami, K., Rainfall-runoff- inundation analysis of the 2010 Pakistan flood in the Kabul River basin, *Hydrological Sciences Journal*, vol. 57, no. 2, pp. 298–312, 2012.
- Zhan, F.B. and Noon, C.E., Shortest path algorithms: An evaluation using real road networks, *Transportation Science*, vol. 32, no. 1, pp. 65–73, 1998.

Biographies

Ko Inoue is a graduate student in Graduate School of Science and Engineering, Hosei University, Japan. He received his B.E. degree from Hosei University in 2023. His research interests include operations research and geographic information science.

Daiki Ito received his B.E. degree from Hosei University in 2023. Currently, he works for LTS Inc. His research interests include operations research and geographic information science.

Daiki Okamura received his B.E. degree from Hosei University in 2023. Currently, he works for Toho System Science Co. Ltd. His research interests include operations research and geographic information science.

Hiroyuki Goto is a professor in the department of Industrial and Systems Engineering, Hosei University, Japan. He received his B.S. and M.S. degrees from The University of Tokyo in 1995 and 1997. He received his D.E. degree from Tokyo Metropolitan Institute of Technology in 2004. His research interests include operations research, geographic information science, and high-performance computing.